energies

Article

Research on Coordinated Control Strategy of DFIG-ES System Based on Fuzzy Control

Jianghong Chen, Teng Yuan *, Xuelian Li, Weiliang Li and Ximu Wang

College of Electrical and New Energy, Three Gorges University, Yichang 443002, China; chenjh97@126.com (J.C.); 13367165429@189.cn (X.L.); m17687970037@163.com (W.L.); wangxm914@163.com (X.W.)
* Correspondence: yt15666619727@163.com; Tel.: +86-19071392206

Abstract: As the penetration rate of wind power systems is rising, which causes the overall system's inertia to decline, the power system's capacity to regulate frequency will be negatively affected. Therefore, this paper investigates the inertia control of doubly fed induction generation, and an energy storage system is installed in the wind farm to respond to the frequency deviation. First, a fuzzy control-based virtual inertia adaptive control strategy is presented. The goal of dynamic adjustment of the virtual inertia coefficient is realized by taking into account the uncertain factors of wind speed and frequency change rate. A recovery strategy based on the energy storage system's level of charge is employed to prevent overcharging and over-discharging of the battery. Then, a weight factor based on frequency deviation is introduced to combine the droop output of the energy storage system with the virtual inertia output of the doubly fed induction generation, and the joint output mode of the wind storage system is determined in each stage of primary frequency regulation. Finally, the simulation verification is performed using the wind storage system simulation model created by MATLAB. The comparison results with other control methods prove that the proposed method is effective.

Keywords: DFIG; ES; fuzzy control; virtual inertia; SOC

check for updates

Citation: Chen, J.; Yuan, T.; Li, X.; Li, W.; Wang, X. Research on Coordinated Control Strategy of DFIG-ES System Based on Fuzzy Control. *Energies* **2023**, *16*, 4770. https://doi.org/10.3390/en16124770

Academic Editors: Antonio Cano-Ortega and Konstantin Suslov

Received: 25 April 2023
Revised: 9 June 2023
Accepted: 12 June 2023
Published: 16 June 2023

1. Introduction

1.1. Motivation and Incitement

The percentage of wind power in the electricity system is gradually rising in light of today's increasingly serious energy and environmental pollution issues [1]. However, a lot of wind power access will result in the phenomenon of insufficient frequency modulation and anti-disturbance ability of the power system, which will substantially create large-scale blackouts due to the extremely unstable wind energy. Therefore, double fed induction generation (DFIG) must incorporate frequency support capabilities, including inertial response and primary frequency modulation, in order to assure the safe and stable operation of large-scale wind power grid-connected systems. The current theoretical study mainly concentrates on DFIG inertial control and primary frequency modulation control to obtain better control effects with regard to the frequency modulation problem of DFIG. In order to ensure the balance and continuity of its power supply, the energy storage device has become a key supporting component of wind power and photovoltaic power generation systems [2]. Moreover, the energy storage battery can achieve a complete balance of system power under any circumstance because of its high control accuracy and fast response speed, and using energy storage (ES) technology to counteract the inertia of wind farms has seen positive application outcomes in recent years and has drawn a lot of interest from specialists and academics.

1.2. Literature Review

In order to reduce system frequency fluctuation caused by wind turbine integration, scholars both at home and abroad have paid close attention to the virtual synchronous generator control strategy [3–5]. The concept of virtual inertia was proposed in [6]; when frequency mutation occurred, a large amount of inertia was virtualized to perform frequency modulation by releasing or storing rotational kinetic energy in the unit. The inertial response temporarily released the kinetic energy stored in the rotating mass to prevent the frequency of initial disturbances from decreasing [7,8]. A comprehensive control scheme combining primary frequency modulation and virtual inertia was proposed in [9–11]. The simulation analysis showed that this method could support system frequency stability, but because the maximum power point tracking (MPPT) of DFIG was compromised, the frequency modulation effect was somewhat diminished.

When the power system's frequency fluctuates, the ES device in the wind power generation system has some inertial support capability. The virtual inertia control of a wind farm, aided by an ES device, cannot only effectively improve wind farm frequency stability but also solve the problem of coordination and communication between each unit in a wind power generation system. In [12], an ES system was used to help the wind turbine increase its inertial response capabilities, which improved the DFIG-ES system's overall ability to regulate frequency but resulted in the second drop in system frequency. In reference [13], ES was implemented in the wind farm's AC bus to reduce frequency fluctuations in the DFIG and so prevent a secondary frequency drop brought on by rotor speed recovery; because ES only supplies the necessary energy during rotor speed recovery or compensates for the insufficient DFIG supply, its enormous potential is underutilized. In order to make full use of wind energy and ES, the authors in [14] suggested a control approach using system frequency deviation and frequency change rate to offer bidirectional active power input. In [15], ES was used only for quick frequency responses, whereas DFIG was run in MPPT mode and did not react to frequency changes. However, these management measures shorten the useful life of ES and raise its maintenance costs. The authors in [16] proposed a serial and parallel optimal control strategy based on a DFIG-ES system, which takes the economy and system frequency modulation performance into account to some extent. Overall, the previous research work does not account for the effect of wind speed variations on the system's frequency modulation effect that can enable DFIG and ES to respond to frequency perturbations to the maximum extent possible at any wind speed.

Combining the advantages and disadvantages of the above literature, the paper is devoted to proposing a frequency modulation method that enables the wind storage system to respond quickly to suppress the system frequency fluctuation when it is disturbed. In addition, the frequency modulation method also needs to make full use of energy storage resources to avoid overcharging and over-discharging, thereby prolonging the service life of energy storage batteries and reducing system costs.

1.3. Contribution and Paper Organization

In this paper, a coordinated control scheme of the DFIG-ES system based on fuzzy control is proposed. In Section 2, a mathematical model of the DFIG-ES system is established. To realize that the virtual inertia coefficient of DFIG can change with wind speed, a fuzzy control method is used for the design in Section 3.1, namely, an adaptive virtual inertia parameter controller that takes wind speed and the system frequency change rate into account. To avoid overcharging and over-discharging of the ES battery while assisting the virtual inertia control of the wind turbine, a state of charge (SOC) ES system recovery strategy is designed in Section 3.2, which keeps the state of charge within a reasonable range, thus extending the service life of the ES battery. To fully utilize wind energy and ES, the joint output mode of the DFIG-ES system is determined in each stage of primary frequency regulation in Section 3.3, and the coordinated operation of the two control methods is achieved. In Section 4, evaluation indexes are given to compare the performance of the simulation results. Finally, based on the simulation model and simulation results of the

DFIG-ES system built by MATLAB, the effectiveness of the proposed method is verified by comparing it with other control methods in Section 5. Table 1 represents all the related variables involved in the paper.

Table 1. Related variables involved in the paper.

Variable	Meaning	Variable	Meaning
f/Hz	Frequency	Q_n/pu	Rated capacity of ES
Δf_m/Hz	Maximum frequency deviation	P_{ES}/pu	Charge and discharge power of ES
t/s	time	v_w/m/s	Wind speed
Δt_m/s	Time for maximum frequency deviation	$d\Delta f/\Delta t$	Frequency change rate
P_{MPPT}/pu	Output power instruction of MPPT control link	I_{BRE}/A	Charge and discharge current of the ES battery
ΔP_v/pu	Active signal of virtual inertial control	Q_{SOC}/pu	SOC value
K_f	Virtual inertia proportional coefficient	ΔQ_{SOC}/pu	SOC deviation
ΔP_c/pu	Power provided by the ES system	ΔP_E/pu	Primary frequency modulation output
$\Delta f(s)$/Hz	Frequency deviation signal at the input signal end of the grid	α, β	Weight factors
k_{pf}	Primary frequency modulation coefficient	$2\Delta f_{set}$/Hz	Set frequency deviation critical value
T_c/s	Response time constant of the ES	ΔP_w/pu	Rotor kinetic energy variation
S_0/%	Initial value of SOC of ES battery	$\Delta\omega_r$/pu	Wind wheel speed variation

2. Model System

2.1. Model System

Figure 1 shows the DFIG-ES primary frequency control model. To provide the same inertia response as the traditional unit, a frequency control link is added to the DFIG active power control connection. To support the steady functioning of the power system frequency, the virtual inertia coefficient is dynamically adjusted using the fuzzy control approach. The ES device is used to assist the wind farm with virtual inertial control during the inertial response stage. The ES system's participation in the frequency modulation process is increasing, which achieves the goal of reducing the ES output, effectively maintaining the ES's SOC and avoiding the phenomenon of battery service life reduction due to overcharging and over-discharging [17]. Simultaneously, it can mitigate the negative impact of ES on the system when SOC exceeds the upper or lower limit.

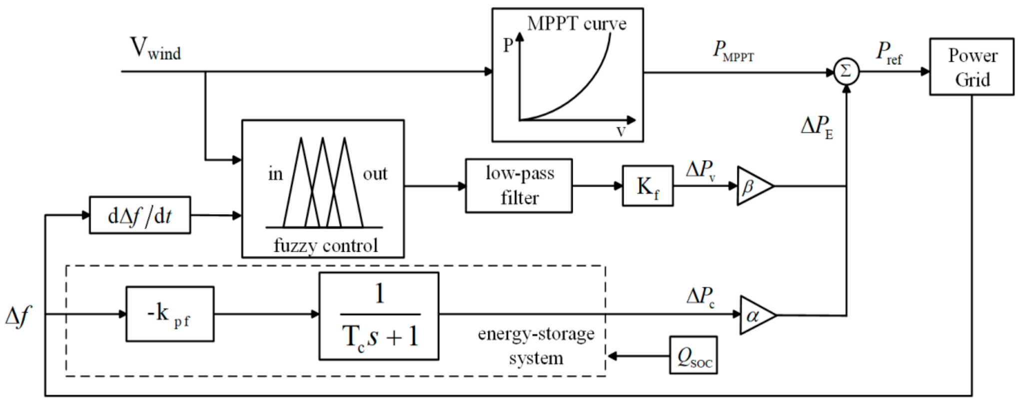

Figure 1. Primary frequency modulation control model of wind energy storage system.

2.2. DFIG System

The control part of DFIG includes an MPPT control part and a frequency modulation control part based on virtual inertia control [18]. The wind turbine output power instruction Pref correspondingly includes two parts, which can be written as follows:

$$P_{ref} = P_{MPPT} + \Delta P_v \tag{1}$$

where P_{MPPT} is the output power instruction of the MPPT control link; ΔP_v is the active signal of virtual inertial control, which can be obtained according to the change rate of system frequency:

$$\Delta P_{\mathrm{v}} = -K_{\mathrm{f}} \mathrm{d}\Delta f / \mathrm{d}t \tag{2}$$

where K_{f} is the proportional coefficient; f is the frequency; t represents time. When the system is disturbed, virtual inertia control can quickly make an active output response by detecting the frequency change.

2.3. ES System

Using the ES system to compensate the virtual inertia control of the wind turbine can improve the energy utilization rate of the ES battery, significantly reduce the power system's rotating reserve capacity, and achieve the goal of lowering the overall system cost [19]. Droop control is commonly used in ES systems to participate in system frequency modulation. The frequency characteristic control model expression of ES can be written as follows:

$$G_{\mathrm{c}}(s) = \Delta P_{\mathrm{c}}(s) / \Delta f(s) = -k_{\mathrm{pf}} / (T_{\mathrm{c}} s + 1) \tag{3}$$

where ΔP_{c} is the power provided by the ES system; $\Delta f(s)$ is the frequency deviation signal at the input signal end of the grid based on the droop control strategy of the ES system; k_{pf} is the primary frequency modulation coefficient; $\mathrm{T_c}$ is the response time constant of the ES.

Since SOC is closely related to parameters such as voltage, current, and internal resistance[20], the power of the ES battery can be described by SOC, which can be written as follows:

$$S_{\mathrm{SOC}} = S_0 - (1/Q_{\mathrm{n}}) \int P_{\mathrm{ES}} \mathrm{d}t \tag{4}$$

where S_0 is the initial value of SOC of ES battery; Q_{n} is the rated capacity of ES; P_{ES} is the charge and discharge power of ES, and the discharge meter is positive. If the SOC is less than the lower limit, the discharge power must be limited within a certain range, but charging is not restricted; if the SOC exceeds the upper limit, the charging power must be limited, but charging is not restricted; and the SOC in the middle area can charge and discharge normally.

3. Proposed Method

3.1. Virtual Inertial Control

The triangular membership function and Mamdani fuzzy controller with a simple form and good control effect were used in this paper, and the centroid method was used to deblur. In this study, the wind speed v_w (7–12.5 m/s) was set as one of the fuzzy controller's input signals, and the frequency change rate $\mathrm{d}\Delta f/\Delta t$ (-1–1 Hz/s) was established as another input signal in accordance with the power system's needs for frequency modulation. The membership functions of input and output signals were examined for seven fuzzy subsets [21]. The fuzzy subsets of $\mathrm{d}\Delta f/\Delta t$ were composed of {NL.NM,NS,Z0,PS,PM,PL}, and the fuzzy subsets of the v_w signal were composed of {FL,FM,FS,F0,ZS,ZM,ZL}. The system will change the virtual inertia proportional coefficient K_f (0.1–1) in real time in response to various wind speed and frequency difference signals in accordance with the planned fuzzy rules, and {VL,ML,SL,M,SH,MH,VH} make up its fuzzy set. The membership functions of input variables and output variables are shown in Figure 2.

Table 2 represents the fuzzy rule, and Figure 3 displays the outcomes of the fuzzy control system's inference. The minimum frequency modulation output (VL) should be used when the DFIG system operates in the low wind speed (FL) region, regardless of the frequency change rate; the active frequency modulation power of the DFIG increases with the increase in wind speed after the wind speed gradually increases to the middle wind speed ranges; the wind turbine can resist larger frequency modulation sharing in the high wind speed (ZL) region; at this point, the upper–middle (MH) level of the DFIG's minimum frequency modulation output is reached, and it is subsequently modified in accordance with the frequency change rate.

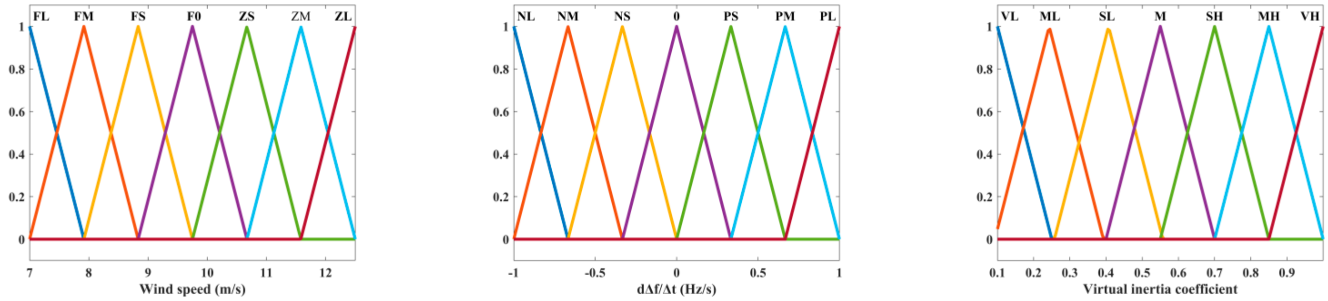

Figure 2. Membership function.

Table 2. Fuzzy logic rules for controller.

K_f		v_w						
		FL	**FM**	**FS**	**F0**	**ZS**	**ZM**	**ZL**
$d\Delta f/\Delta t$	NL	VL	M	SH	MH	VH	VH	VH
	NM	VL	SL	M	MH	VH	VH	VH
	NS	VL	SL	M	SH	VH	VH	VH
	Z0	VL	ML	SL	SH	MH	VH	VH
	PS	VL	ML	SL	M	MH	MH	VH
	PM	VL	VL	ML	SL	SH	MH	MH
	PL	VL	VL	ML	SL	M	SH	MH

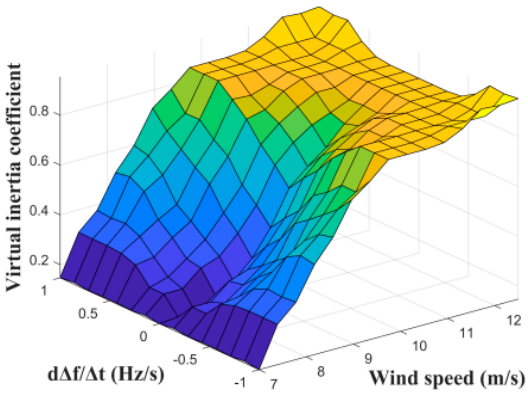

Figure 3. Result of fuzzy logic inference of fuzzy control.

3.2. SOC Recovery Strategy

Although the operation of the ES system can compensate for the virtual inertia control of the wind turbine to some extent, it can also prevent the occurrence of dangerous conditions such as the secondary drop in grid frequency [22,23], However, because the current energy storage application scale is still very small relative to the grid capacity, if the maximum power coefficient is always used, the limit of the SOC of energy storage is easily exceeded. In order to solve this problem, the output of energy storage can be appropriately reduced when the SOC is too high or too low, or the charging and discharging coefficient of energy storage can be dynamically adjusted to achieve the purpose of reducing the output of energy storage. On the one hand, it can make the energy storage better maintain the SOC and prevent the energy storage battery from overcharging and over-discharging affecting the battery service cycle; on the other hand, it can effectively avoid the adverse effects of energy storage on the system when the SOC exceeds the limit.

Based on the introduction of inertial control [24], this paper charged and discharged the energy storage battery, simplified its control function, and made the adaptive control law achieve a better frequency regulation effect. As a result, this paper divided SOC into five regional ranges: [0, 0.1], [0.1, 0.3], [0.3, 0.7], [0.7, 0.9], and [0.9, 1]. When the frequency deviation amplitude is within the set frequency deviation threshold range and the Qsoc exceeds the set SOC upper limit or upper limit, the SOC recovery signal is triggered, and the constant current charge and discharge will be performed according to the following formula to achieve SOC recovery:

$$I_{\mathrm{BRE}} = \begin{cases} 1, & Q_{\mathrm{SOC}} \in [0.7, 1] \\ (Q_{\mathrm{SOC}} - 0.6)/0.1, & Q_{\mathrm{SOC}} \in [0.6, 0.7] \\ 0, & Q_{\mathrm{SOC}} \in [0.4, 0.6] \\ (0.4 - Q_{\mathrm{SOC}})/0.1, & Q_{\mathrm{SOC}} \in [0.3, 0.4] \\ -1, & Q_{\mathrm{SOC}} \in [0, 0.3] \end{cases} \tag{5}$$

where I_{BRE} is the charge and discharge current of the ES battery during SOC recovery, and Q_{SOC} is the SOC value.

3.3. Coordinated Control

Considering that the virtual inertia control has a better suppression effect on dΔf, and the ES system droop control has a better suppression effect on Δf, the weight factor was introduced to balance the output ratio of the two control methods and enable the DFIG-ES to participate in the primary frequency modulation process of the power grid [25,26]. The virtual inertia output of the wind power system and the droop output of the ES system make up the primary frequency regulation output of the DFIG-ES at any given time, which can be written as follows:

$$\Delta P_{\mathrm{E}} = \alpha \Delta P_{\mathrm{c}} + \beta \Delta P_{\mathrm{v}} \tag{6}$$

where ΔP_{E} is the primary frequency modulation output of DFIG-ES, and α and β are the weight factors for the primary frequency modulation droop output and virtual inertia output, respectively. The output ratio of the droop output and virtual inertial output must be configured sensibly and flexibly in order to satisfy the power grid's requirements for frequency regulation. Because of this, this paper designed the frequency deviation, which can be expressed as follows:

$$\alpha = \begin{cases} 0.5 + |\Delta f|/(2\Delta f_{\mathrm{set}}) & 0 \le |\Delta f| \le 2\Delta f_{\mathrm{set}} \\ 1.5 & |\Delta f| \ge 2\Delta f_{\mathrm{set}} \end{cases} \tag{7}$$

$$\beta = \begin{cases} 1.5 - |\Delta f|/(2\Delta f_{\mathrm{set}}) & 0 \le |\Delta f| \le 2\Delta f_{\mathrm{set}} \\ 0.5 & |\Delta f| \ge 2\Delta f_{\mathrm{set}} \end{cases} \tag{8}$$

where $2\Delta f_{\mathrm{set}}$ is the set frequency deviation critical value. Based on the frequency deviation, the system can reasonably control the droop output of the ES system and the proportion of the virtual inertia output of the DFIG. When the frequency deviation is small, the proportion of the virtual inertia output is increased to achieve the goal of system stabilization. In the case of a large frequency deviation, the proportion of the ES system's droop output is increased to achieve the goal of rapid frequency recovery.

4. Evaluating Indicator

In this paper, the maximum frequency deviation Δf_{m} and its corresponding response time Δt_{m} were used to evaluate the control strategy's frequency modulation effect [27], and the SOC deviation ΔQ_{SOC} after 200 s of long-term charge and discharge was used to evaluate the control strategy's SOC maintenance effect. The lower the Δf_{m} value, the better the frequency modulation effect; the smaller the Δt_{m}, the faster the frequency response capability, the stronger the grid frequency modulation capability, and the better the grid frequency stability. The smaller the amplitude of ΔQ_{SOC}, the better the control strategy's SOC maintenance effect.

5. Simulation Results

5.1. The Dynamic Response at Different Wind Speeds

The simulation platform in this paper was built using MATLAB(R2021a)/Simulink software. The power supply for the simulation system had an installed capacity of 600 MW, with the wind power penetration rate set to 25% and the initial value of the state of charge set to 0.8.

Figure 4 shows the adaptive fluctuation curve of virtual inertia coefficient under wind speed. The virtual inertia coefficient varied in response to wind speed. The virtual inertia coefficient was intended to be larger at high wind speeds to allow the DFIG to release more kinetic energy in the case of a rapid reduction in system frequency; the virtual inertia coefficient was set to be smaller at low wind speeds to maintain steady operation of the DFIG. Therefore, the control strategy suggested in this paper could dynamically adjust the virtual inertia coefficient in accordance with the change in wind speed, ensuring the smooth and reliable operation of the DFIG in the frequency regulation process under low wind speed conditions while also enhancing its capability to support frequency under operating conditions of high wind speed.

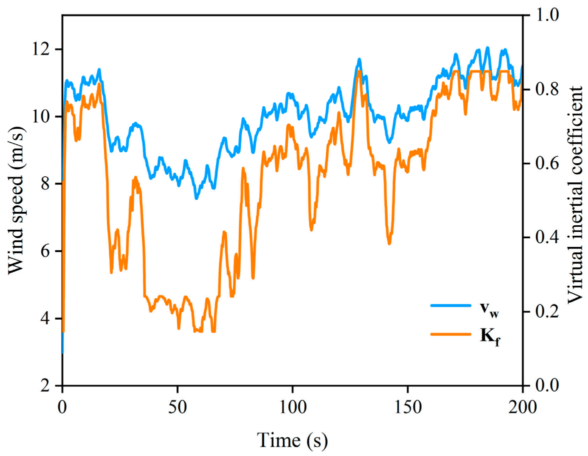

Figure 4. The adaptive fluctuation curve of virtual inertia coefficient under simulated wind speed.

Figure 5 and Table 3 show the comparative curves of DFIG frequency variations for different wind speeds, namely, 12 m/s (strong wind), 10 m/s (medium wind), and 8 m/s (low wind), under the control strategy proposed in this paper. During the simulation run up to 400 s, there was a load step disruption of 0.1 pu. The system frequency decreased by 0.27 Hz at the low wind speed zone (8 m/s), where the simulation was run for up to 400.85 s. The virtual inertia parameter was set to only 0.17 to guarantee reliable functioning of the turbine in the low wind speed region. When a medium wind speed signal (10 m/s) was provided, the simulation reduced the system frequency by 0.23 Hz at 400.95 s and increased the virtual rotational inertia parameter to 0.6. When the DFIG was run in the high wind speed region (12 m/s), the system frequency only dropped by 0.194 Hz after the simulation was runs to 401.14 s, and its virtual rotational inertia parameter was raised to 0.85. The fuzzy variable parameter virtual inertia control strategy proposed in this paper could effectively compensate the inertia of the wind power system under different wind speed conditions and improve the system's frequency operation characteristics.

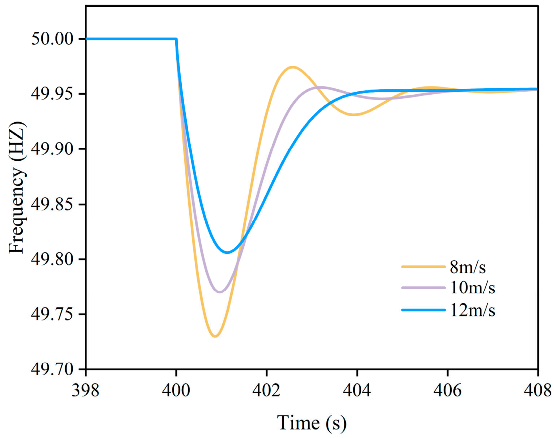

Figure 5. Frequency response curves of the system with different wind speeds.

Table 3. Comparison of different wind speeds.

Wind Speeds	Δf/Hz	Δt/s	K_f
8 m/s	0.27	0.85	0.17
10 m/s	0.23	0.95	0.6
12 m/s	0.194	1.14	0.85

5.2. System Dynamic Response during Load Surges

The generation and load were dynamically balanced at the initial moment; the system frequency was 50 Hz, and the input wind speed was set to 9 m/s. At 400 s, a load step disturbance of 0.1 pu occurred in the system. The proposed control strategy in the paper was compared with other three reported strategies: Case 1, wind power system without frequency modulation [28]; Case 2, wind power system with fixed virtual inertia coefficient frequency modulation [29]; Case 3, frequency modulation with fixed output ratio fuzzy control [30]; and Case 4, the proposed control.

Figure 6 and Table 4 show that when the DFIG did not take part in grid frequency regulation, it did not need to provide active support through energy output, so its speed was constant. When the DFIG took part in frequency regulation, regardless of whether the virtual rotational inertia parameter was constant or dynamical, as long as the DFIG was in a stable working condition, it released the kinetic energy of the rotor by reducing the speed of the wind wheel, thereby providing energy support for the system power. The fuzzy control method proposed in this paper reduced the speed variation to 0.7393 pu during the DFIG frequency dynamics, thus enabling the DFIG to rapidly increase the active output to 0.218 pu, which played a significant role in inertial support for the system.

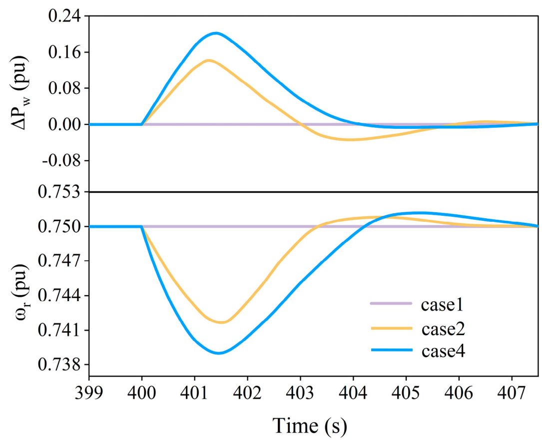

Figure 6. Dynamic response curves of the system under different control strategies.

Table 4. Comparison of different control strategies.

Control Strategies	ΔP_w/pu	$\Delta \omega_r$/pu	Δf_m/Hz	Δt_m/s	ΔQ_{SOC}
Case 1	0	0	0.3792	0.900	-
Case 2	0.152	7.5×10^{-3}	0.3652	0.910	-
Case 3	-	-	0.2449	1.025	0.5684
Case 4	0.218	10.8×10^{-3}	0.1938	1.144	0.4260

Figure 7 and Table 4 show that the DFIG-ES frequency rapidly decreased to its lowest point when the wind power system was not engaged in frequency modulation, with a peak frequency deviation of 0.3792 Hz and a frequency drop speed of 0.4210 Hz/s. The DFIG participated in frequency regulation for the other three frequency control methods, lowering the lowest point and speed of the system frequency drop. A peak frequency deviation of only 0.1938 Hz and a drop speed of only 0.1694 Hz/s were shown to have damped the system's frequency change rate to some extent over time, further enhancing the system's frequency characteristics and successfully suppressing the frequency deviation. When compared to the other three primary frequency modulation control methods, the proposed frequency modulation control technique may also have alleviated the secondary frequency drop, allowing the system frequency to reach the required level of 0.2 Hz more quickly.

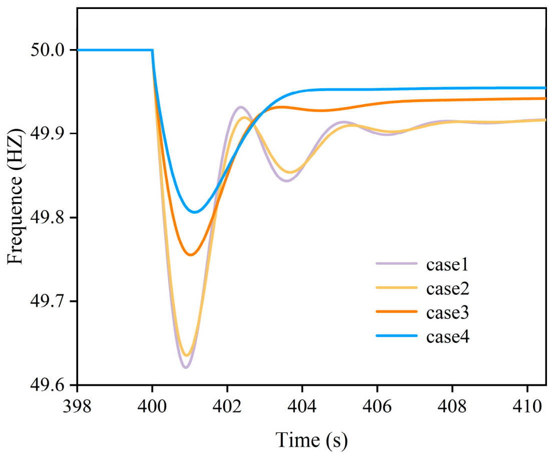

Figure 7. Frequency response curves of the system with different control strategies.

Figure 8 and Table 4 show that when using the fixed output ratio fuzzy control frequency modulation strategy, the SOC deviation amplitude was 0.5684 after the 400 s step load disturbance, which consumed more power, had a poor SOC maintenance effect, and easily caused the ES battery to overcharge and over-discharge; in contrast, when using the strategy of this paper, the ΔQ_{SOC} deviation amplitude was 0.426, which consumed less power, indicating that the SOC maintenance effect was the best; however, the response time was slightly longer, and the maximum frequency deviation of Δf_{m} was significantly lower than the other methods, suppressing the significant drop in frequency.

It should be noted that the above simulation experiments could demonstrate the effectiveness of the coordination control strategy suggested in this paper because the step change operations were the most hazardous conditions for the system, and if the system performance parameters could meet the requirements under these condition, they could also meet the requirements under other disturbance conditions.

Because this paper only interfered with the system under fixed wind speed, the comparison waveform of each variable of the system under different frequency modulation strategies was obtained, and only the simulation comparison of the system frequency under different wind speed modes. Next, we will carry out a simulation comparison of other variables in the system under different wind speed modes to better verify the applicability of the control strategy proposed in this paper in the actual situation of wind power grid operation and control.

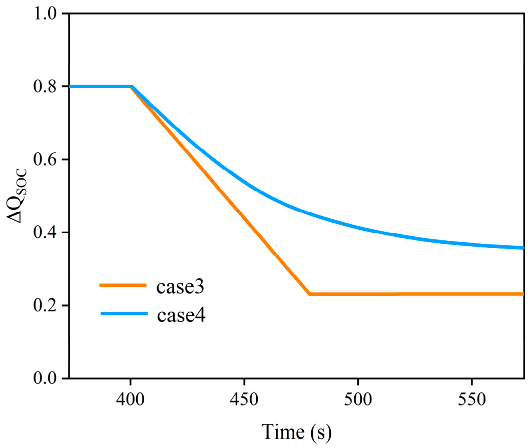

Figure 8. SOC waveform curves under different control strategies.

6. Conclusions

The dynamic stability of the system frequency will be impacted as more wind power is put into use, as will a weakening of the system's moment of inertia. In this study, it is suggested that a coordinated DFIG-ES control method based on fuzzy control can somewhat increase the wind power generating system's capacity for frequency support. The following results are drawn from a simulation analysis of several control strategies.

The adaptive fuzzy control approach proposed in this study allows the virtual inertia coefficient to be dynamically modified according to wind speed fluctuations, resulting in smooth DFIG operation at low wind speeds and adequate energy support at high wind speeds.

The DFIG-ES coordinated control strategy can better respond to frequency changes and enhance the primary frequency modulation capability of the DFIG, achieving the objectives of improving the frequency response characteristics of the system and lowering the steady-state frequency difference of the wind storage system.

The strategy proposed in this paper differs from traditional DFIG inertia control strategies in that it allows the DFIG and the ES system to complement each other. The SOC is also kept within a reasonable range by using weighting factors to control the proportion of the ES system's droop output and virtual inertia output, it improves the utilization rate of energy storage battery, and it has certain reference value for prolonging the service life of the energy storage battery and reducing system costs.

7. Discussion

In this paper, the traditional primary frequency modulation method of a wind storage system is optimized, and a coordinated control strategy based on fuzzy control of a wind storage system is proposed, which achieved certain results. To further test the effectiveness of the proposed method, the coordinated control strategy proposed in this paper can subsequently be used to simulate and analyze different types of working conditions such as random load disturbance conditions and transient short circuit fault conditions. In addition, there are still some areas for improvement in this control strategy. For example, it will still cause secondary fluctuations in the system frequency. Subsequently, the secondary frequency modulation method of the DFIG-ES system can be studied.

Author Contributions: Conceptualization, methodology, and guide modification, J.C.; writing—original draft preparation, modeling, and simulation, T.Y.; methodology, X.L.; translation, W.L.; translation and modify, X.W. All authors have read and agreed to the published version of the manuscript.

Funding: This research received no external funding.

Data Availability Statement: The data presented in this study are available upon request from the corresponding authors. The data are not publicly available due to privacy.

Conflicts of Interest: The authors declare no conflict of interest.

Abbreviations

Abbreviation	Full Name
DFIG	Double fed induction generation
ES	Energy storage
MPPT	Maximum power point tracking
SOC	ES system state of charge

References

1. Ahmed, M.; Abderrezak, G.; Hocine, B.; Adel, M. New neural network and fuzzy logic controllers to monitor maximum power for wind energy conversion system. *Energy* **2016**, *106*, 137–146.
2. Ayyarao, T.S.L.V.; Ayyarao, V. Modified vector controlled DFIG wind energy system based on barrier function adaptive sliding mode control. *Prot. Control. Mod. Power Syst.* **2019**, *4*, 34–41. [CrossRef]
3. Han, J.; Liu, Z.; Liang, N. Nonlinear adaptive robust control strategy of doubly fed induction generator based on virtual synchronous generator. *IEEE Access* **2020**, *8*, 159887–159896. [CrossRef]
4. Peng, B.; Zhang, F.; Liang, J.; Ding, L.; Liang, Z.; Wu, Q. Coordinated control strategy for the short-term frequency response of a DFIG-ES system based on wind speed zone classification and fuzzy logic control. *Int. J. Electr. Power Energy Syst.* **2019**, *107*, 363–378. [CrossRef]
5. Cao, Y.; Wang, W.; Li, Y.; Tan, Y.; Chen, C.; He, L.; Häger, U.; Rehtanz, C. A virtual synchronous generator control strategy for VSC-MTDC systems. *IEEE Trans. Energy Convers.* **2017**, *33*, 750–761. [CrossRef]
6. Hurtado, S.; Gostales, G.; De Lara, A.; Moreno, N.; Carrasco, J.M.; Galvan, E.; Sanchez, J.A.; Franquelo, L.G. A new power stabilization control system based on making use of mechanical inertia of a variable-speed wind-turbine for stand-alone wind-diesel applications. In Proceedings of the IEEE 2002 28th Annual Conference of the Industrial Electronics Society, Seville, Spain, 5–8 November 2002; Volume 9, pp. 3326–3331.
7. Ghosh, S.; Kamalasadan, S.; Senroy, N.; Enslin, J. Doubly fed induction generator (DFIG)-based wind farm control framework for primary frequency and inertial response application. *IEEE Trans. Power Syst.* **2015**, *31*, 1861–1871. [CrossRef]
8. Chen, T.; Feng, D.; Wu, X.; Lu, C.; Xu, B. Modeling and stability analysis of interaction between converters in AC-DC distribution systems. *Front. Energy Res.* **2023**, *10*, 1035193. [CrossRef]
9. Cui, S.; Yan, X.; Siddique, A. Inertia and primary frequency modulation strategy for a doubly fed induction generator based on supercapacitor energy storage control. *Int. J. Green Energy* **2022**, *19*, 941–955. [CrossRef]
10. Xin, H.; Liu, Y.; Wang, Z.; Gan, D.; Yang, T. A new frequency regulation strategy for photovoltaic systems without energy storage. *IEEE Trans. Sustain. Energy* **2013**, *4*, 985–993. [CrossRef]
11. Yuan, X.; Li, Y. Control of variable pitch and variable speed direct-drive wind turbines in weak grid systems with active power balance. *IET Renew. Power Gener.* **2014**, *8*, 119–131. [CrossRef]
12. Jiang, W.; Lu, J.; Mei, Y. Study on frequency control strategy of wind farm-energy storage system. *ICIC Express Lett.* **2015**, *9*, 2657–2663.
13. Qu, L.; Wei, Q. Constant power control of DFIG wind turbines with supercapacitor energy storage. *IEEE Trans. Ind. Appl.* **2010**, *47*, 359–367. [CrossRef]
14. Zhang, S.; Yateendra, M.; Mohammad, S. Fuzzy-logic based frequency controller for wind farms augmented with energy storage systems. *IEEE Trans. Power Syst.* **2015**, *31*, 1595–1603. [CrossRef]
15. Miao, L.; Wen, J.; Xie, H.; Yue, C.; Lee, W.J. Coordinated control strategy of wind turbine generator and energy storage equipment for frequency support. *IEEE Trans. Ind. Appl.* **2015**, *51*, 2732–2742. [CrossRef]
16. Li, C.; Zhang, Z.; Li, J.; Ma, Y.; Zou, J. Design of Control Strategy and Effect Evaluation for Primary Frequency Regulation of Wind Storage System. *Front. Energy Res.* **2021**, *9*, 739439. [CrossRef]
17. Hua, X.; Xu, H.; Li, N. Control strategy of DFIG wind turbine in primary frequency regulation. In Proceedings of the 2018 13th IEEE Conference on Industrial Electronics and Applications (ICIEA), Wuhan, China, 31 May–2 June 2018; Volume 5, pp. 1751–1755.
18. Peng, Z.; Wang, J.; Wen, Y.; Bi, D.; Dai, Y.; Ning, Y. Virtual synchronous generator control strategy incorporating improved governor control and coupling compensation for AC microgrid. *IET Power Electron.* **2019**, *12*, 1455–1461. [CrossRef]
19. Tu, S.; Zhang, B.; Jin, X. Research on DFIG-ES system to enhance the fast-frequency response capability of wind farms. *Energies* **2019**, *12*, 3581. [CrossRef]
20. Pandzic, H.; Bobanac, V. An Accurate Charging Model of Battery Energy Storage. *IEEE Trans. Power Syst.* **2019**, *34*, 1416–1426. [CrossRef]

21. Zheng, Z.; Yang, Z.; Li, W. Analysis and comparison of primary frequency control technology for wind power and thermal power unit. *Electr. Power Autom. Equip.* **2017**, *37*, 92–101.
22. Mohammad, D.; Mokhlis, H.; Mekhilef, S. Inertia response and frequency control techniques for renewable energy sources: A review. *Renew. Sustain. Energy Rev.* **2017**, *69*, 144–155.
23. Vidyanandan, K.V.; Senroy, N. Primary Frequency Regulation by Deloaded Wind Turbines Using Variable Droop. *IEEE Trans. Power Syst.* **2013**, *28*, 837–846. [CrossRef]
24. Liu, J.; Yao, W.; Wen, J.; Ai, X.; Luo, W.; Huang, Y. A wind farm virtual inertia compensation strategy based on energy storage system. *Chin. J. Electr. Eng.* **2015**, *35*, 1596–1605.
25. Zhou, Q.; Wang, C.; Bu, J. Coordinated control strategy for improving the two drops of the wind storage combined system. *IOP Conf. Ser. Earth Environ. Sci.* **2018**, *153*, 022041. [CrossRef]
26. Zhao, J.; Li, M.; He, X.; Zhu, R. Coordinated Control Strategy of Wind Power and Energy Storage in Frequency Regulation Based on Torque Limit Control. *Trans. China Electrotech. Soc.* **2019**, *34*, 4982–4990.
27. Li, J.; Ma, H.; Yuan, X.; Wang, Z.; Ge, L. Overview on Key Applied Technologies of Large-Scale Distributed Energy Storage. *Power Grid Technol.* **2017**, *41*, 3365–3375.
28. Lu, M.S.; Chang, C.L.; Lee, W.J.; Wang, L. Combining the Wind Power Generation System with Energy Storage Equipment. *IEEE Trans. Ind. Appl.* **2009**, *45*, 2109–2115.
29. Gevorgian, V.; Zhang, Y.; Ela, E. Investigating the Impacts of Wind Generation Participation in Interconnection Frequency Response. *IEEE Trans. Sustain. Energy* **2015**, *6*, 1004–1012. [CrossRef]
30. Zhao, H.; Hong, M.; Lin, W.; Loparo, K.A. Voltage and Frequency Regulation of Microgrid With Battery Energy Storage Systems. *IEEE Trans. Smart Grid* **2019**, *10*, 414–424. [CrossRef]